ORNL-TM-4271

HOME

HELP

23,122

MASS TRANSFER BETWEEN HASTELLOY N AND A MOLTEN SODIUM FLUOROBORATE MIXTURE IN A THERMAL CONVECTION LOOP

J. W. Koger

MASTER

OAK RIDGE NATIONAL LABORATORY

OPERATED BY UNION CARBIDE CORPORATION • FOR THE U.S. ATOMIC ENERGY COMMISSION

ORNL-TM-4271

Contract No. W-7405-eng-26

METALS AND CERAMICS DIVISION

MASS TRANSFER BETWEEN HASTELLOY N AND A MOLTEN SODIUM FLUOROBORATE MIXTURE IN A THERMAL CONVECTION LOOP

J. W. Koger

DECEMBER 1972

OAK RIDGE NATIONAL LABORATORY
Oak Ridge, Tennessee 37830
operated by
UNION CARBIDE CORPORATION
for the
U.S. ATOMIC ENERGY COMMISSION

CONTENTS

MASS TRANSFER BETWEEN HASTELLOY N AND A MOLTEN SODIUM FLUOROBORATE MIXTURE IN A THERMAL CONVECTION LOOP

J. W. Koger

ABSTRACT

We showed that temperature-gradient mass transfer occurred in a Hastelloy N thermal convection loop circulating a sodium fluoroborate–sodium fluoride mixture ($NaBF_4$–8 mole % NaF) at temperatures of 687°C maximum and 438°C minimum for 19,930 hr. The maximum calculated corrosion rate (based on uniform removal) was 0.29 mil/year. Overall, the compatibility in this system was quite good. Impurities such as air inadvertently admitted to the loop system increased the mass transfer rate. Material (chromium, iron, and nickel) removal resulted in voids in the hot leg. Iron and nickel deposited in the cold section, but chromium ions remained in the salt. Some of the deposits in the cold leg appeared to have cubic symmetry.

1. INTRODUCTION

A thermal convection loop, designated NCL-20 and similar to that pictured in the foreground of Fig. 1, began operation in December 1969 and was drained in March 1972, after 19,930 hr at design conditions. The purpose of the test was to determine the compatibility of standard Hastelloy N with a sodium fluoroborate–sodium fluoride eutectic mixture, $NaBF_4$–8 mole % NaF, at the most extreme temperature conditions considered (687°C maximum and 438°C minimum) for the molten-salt breeder reactor (MSBR) secondary circuit. The temperature extremes are the estimated wall temperatures in the secondary circuit of an MSBR.

The corrosion of Hastelloy N by the sodium fluoroborate mixture has been studied for several years in both thermal convection and pumped loops but usually at temperatures of 610°C and lower.[1–13] The experiment discussed in this report was conducted to determine the mass transfer characteristics at higher temperatures with a larger temperature gradient.

2. EXPERIMENTAL DETAILS

The test system consisted of a thermal convection loop in a harp configuration, with surge tanks atop each leg for sample and specimen access. Flow was generated by the difference in density of the salt in the hot and cold legs of the loop, and the salt flow velocity was approximately 7 ft/min. The loop was operated

1. J. W. Koger and A. P. Litman, *Compatibility of Hastelloy N and Croloy 9M with $NaBF_4$-NaF-KBF_4 (90-4-6 Mole %) Fluoroborate Salt,* ORNL-TM-2490 (April 1969).
2. J. W. Koger and A. P. Litman, *Catastrophic Corrosion of Type 304 Stainless Steel in a System Circulating Fused Sodium Fluoroborate,* ORNL-TM-2741 (January 1970).
3. J. W, Koger and A. P. Litman, *Compatibility of Fused Sodium Fluoroborates and BF_3 Gas with Hastelloy N Alloys,* ORNL-TM-2978 (June 1970).
4. J. W. Koger, *Corrosion and Mass Transfer Characteristics of $NaBF_4$-NaF (92-8 Mole %) in Hastelloy N,* ORNL-TM-3866 (October 1972).
5. J. W. Koger and A. P. Litman, *MSR Program Semiannu. Progr. Rep. Feb. 29, 1968,* ORNL-4354, pp. 221–25.
6. J. W. Koger and A. P. Litman, *MSR Program Semiannu. Progr. Rep. Aug. 31, 1968,* ORNL-4434, pp. 264–66 and 285–89.
7. J. W. Koger and A. P. Litman, *MSR Program Semiannu. Progr. Rep. Feb. 28, 1969,* ORNL-4369, pp. 246–53.
8. J. W. Koger and A. P. Litman, *MSR Program Semiannu. Progr. Rep. Aug. 31, 1969,* ORNL-4449, pp. 200–208.
9. J. W. Koger, *MSR Program Semiannu. Progr. Rep. Feb. 28, 1970,* ORNL-4548, pp. 242–52 and 265–72.
10. J. W. Koger, *MSR Program Semiannu. Progr. Rep. Aug. 31, 1970,* ORNL-4622, pp. 168–78.
11. J. W. Koger, *MSR Program Semiannu. Progr. Rep. Feb. 28, 1971,* ORNL-4676, pp. 192–215.
12. J. W. Koger, *MSR Program Semiannu. Progr. Rep. Aug. 31, 1971,* ORNL-4728, pp. 138–53.
13. J. W. Koger, *MSR Program Semiannu. Progr. Rep. Feb. 29, 1972,* ORNL-4782, pp. 174–82.

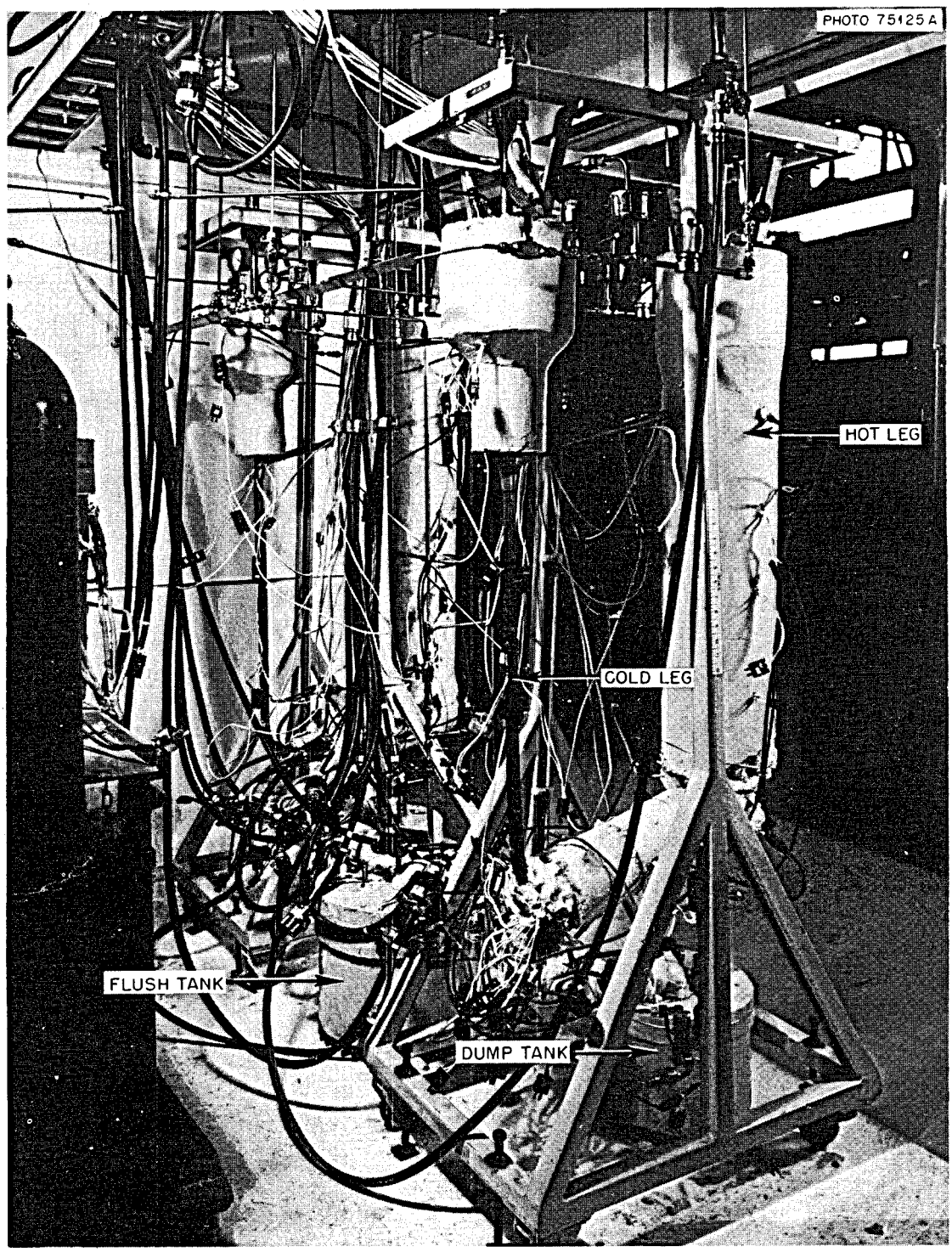

Fig. 1. Hastelloy N thermal convection loop NCL-20 containing $NaBF_4$–8 mole % NaF at a maximum temperature of 687°C with a temperature difference of 249°C.

at a maximum temperature of 687°C and a temperature difference of 249°C. Forced air cooling of the cold leg was required to obtain this ΔT. A schematic of the loop is given in Fig. 2.

2.1 Materials

The harp portion of the loop system was fabricated from 0.750-in. OD, 0.072-in. wall Hastelloy N tubing. This material was part of heat 5095, which was purchased from Wall Tube and Metal Products Company, Newport, Tennessee. The Oak Ridge National Laboratory Inspection Engineering identification number is IR-8402-2. The finished loop system was stress relieved at 900°C for 6 hr in hydrogen.

The loop contained 14 standard Hastelloy N specimens and two titanium-modified Hastelloy N specimens 0.75 X 0.38 X 0.030 in., each with a surface area of 0.55 in.^{2} (3.5 cm^2). Modifications to the standard Hastelloy N composition are being made to test for improved mechanical properties after irradiation and were included in this test to check their compatibility with the sodium fluoroborate mixture. The compositions of the standard and modified Hastelloy N specimens are given in Table 1. Eight specimens were attached at different vertical positions on each of two $\frac{1}{8}$-in. rods. One rod was inserted in the hot leg and another in the cold leg. The rods were placed into or removed from the loop from standpipes atop each leg. The rods were moved through a Teflon sliding seal compression fitting at the top of the standpipe and a ball valve at the bottom. Another ball valve on the loop above each leg assured removal or insertion without disturbing loop operation or introducing air contamination.

Table 1. Nominal compositions of corrosion specimens

In percent by weight

	Cr	Fe	Mo	Ni	Ti
Standard Hastelloy N	7.4	4.5	17.2	70.0	0.02
Ti-modified Hastelloy N	7.3	<0.1	13.6	77.0	0.5

2.2 Salt Preparation

The fluoroborate salt mixture was furnished by the Fluoride Processing Group of the Reactor Chemistry Division, and its composition before test is given in Table 2. To mix and purify the salt, the raw materials were first heated in a nickel-lined vessel to 150°C under vacuum and held for 15 hr. Then the salt was heated to 500°C, agitated with helium for a few hours, and transferred to the fill vessel.

Table 2. Salt analysis before test

Element	Content (%)	Element	Content (ppm)
Na	21.4	Cr	58
B	9.47	Ni	5
F	68.4	Fe	227
		0	600
		Mo	2

2.3 Loop Operation

The loop was heated by pairs of clamshell heaters placed end to end, with the input power controlled by silicon controlled rectifier units and the temperature controlled by a current-proportioning controller.

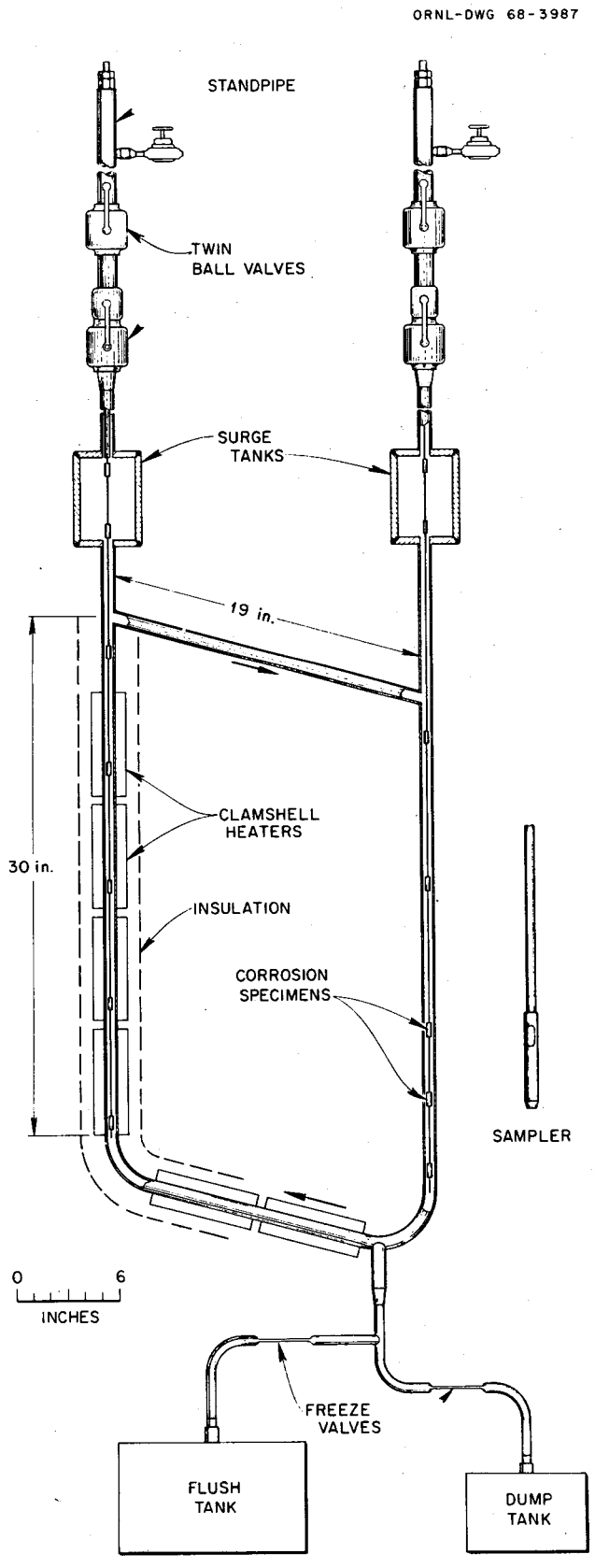

Fig. 2. MSRP natural circulation loop and salt sampler.

Temperatures were measured by Chromel-P vs Alumel thermocouples that were spot welded to the outside of the tubing, covered by a layer of quartz tape, and then covered with stainless steel shim stock. Tubular electric heaters controlled by variable autotransformers furnished the heat to the cold leg portions of the loops.

Before filling with salt, the loop was degreased with ethyl alcohol, dried, and then heated to 150°C under vacuum to remove any traces of moisture. A helium mass spectrometer leak detector was used to check for leaks in the system.

The loop was filled by heating the harp section, the salt pot, and all connecting lines to approximately 550°C and applying helium pressure to the salt supply vessel to force the salt into the system. Air was continuously blown on freeze valves leading to the dump and flush tanks to provide a positive salt seal. All fill lines exposed to the fluoroborate salt were Hastelloy N, and all temporary connections from fill line to loop were made with stainless steel compression fittings.

A flush salt charge, intended to remove surface oxides and other impurities, was held for 24 hr in the loop at the maximum operation temperature and then dumped. The loop was then refilled with fresh salt. Once the loop was filled, the heaters on the cold leg of the loop were turned off. As much insulation as necessary was removed to obtain the proper temperature difference by exposing the cold leg to ambient air. Helium cover gas of 99.998% purity and at a slight positive pressure (approx 5 psig) was maintained over the salt during operation.

Corrosion specimens were withdrawn periodically along with salt samples to follow corrosion processes as a function of time. During the removal periods, all specimens were weighed and measured. Portions of the hottest and coldest specimens were removed and examined metallographically during test, and all specimens were examined metallographically after test. After the end of the experiment, the hottest and coldest specimens were analyzed by scanning electron microscopy (SEM) and x-ray fluorescence. The x-ray fluorescence was induced by bombardment by the electron beam of the SEM.

3. RESULTS

3.1 Operation, Weight Changes, and Salt Chemistry

For the first 11,900 hr, weight-change measurements showed losses in specimens from the hot section and gains from those in the cold section. The maximum weight loss was 6.2 mg/cm^2 (corrosion rate 0.2 mil/year, assuming uniform removal), and the maximum gain was 2.8 mg/cm^2. Table 3 gives the weight loss of the hottest specimen and the concentration of the major impurities in the salt as a function of time.

Table 3. Weight change of specimen at 687°C and impurity content of salt of NCL-20

Time (hr)	Maximum weight loss (mg/cm^2)	Incremental corrosion rate (mils/year)[a]	Chemical analysis (ppm)		
			Cr	Fe	Oxide
0			58	227	900
624	0.3	0.19	90	198	550
1,460	0.7	0.18	99	110	590
2,586	1.0	0.15	109	104	470
3,784	1.7	0.17	131	91	670
8,500	4.3	0.2	175	90	550
11,900	6.2	0.2	198	90	720

[a]Assuming uniform loss.

Operation of the loop was uneventful during these 11,900 hr, and the weight changes of the specimens and the chemistry changes of the salt indicated that the mass transfers were the lowest attained yet with the fluoroborate mixture in a temperature gradient system. At 12,429 hr the normal 20-psia helium overpressure dropped to atmospheric pressure. Investigation disclosed that the safety valve on the helium regulator had failed and had released helium from the loop. To determine if the salt had become contaminated with air or moisture, the specimens were immediately removed from the loop and weighed. The maximum metal loss during this additional time period (525 hr) was fairly low (0.34 mil/year) with a correspondingly low weight gain on cold leg specimens. Thus, the mass transfer rate increased but did not greatly accelerate. A salt analysis did not disclose any gross changes. The distance from the regulator to the loop was approximately 20 ft, and the gas line was $\frac{1}{4}$-in. tubing; therefore, movement of air into the loop system was somewhat difficult but not impossible. The valve was replaced, and loop operation continued.

During the next 1850 hr, the maximum corrosion rate (assuming uniform loss) was 0.7 mil/year. Part of this increased mass transfer was associated with the regulator problem and some impurity inleakage, but further inspection disclosed a leaking mechanical pressure fitting. The fitting was repaired, and the loop continued operation.

During the last few hundred hours of operation, variations in flow were noted. The specimens were removed and the salt was frozen in the loop. On removal of the heaters we found that the loop tubing had been severely damaged and pitted because of direct contact with the heater wire. The insulator bushing normally used to separate the heater and the tubing had slipped out of place. We decided to make repairs by weld overlaying Hastelloy N on the damaged portions of the tubing. Because of the possibility of penetration through the tubing while overlaying, the heaters were temporarily wired back in place and the loop was drained. This terminated the operation of NCL-20 after 19,930 hr of operation.[14]

Table 4 lists the specimens, their position in the loop, the temperature of the salt at the various positions, thickness measurements, and weight changes after 19,300 hr exposure time. The specimens in the hottest position showed the greatest loss, 14.4 mg/cm^2 for the standard Hastelloy N and 15.5 mg/cm^2 for the modified Hastelloy N. The maximum corrosion rate (assuming uniform loss) was 0.29 mil/year. The maximum weight gain in the cold leg was 4.0 mg/cm^2. Thickness measurements were made before and after test, and the changes in thickness corresponded quite well to the weight changes, that is, weight losses were associated with decreases in thickness and weight gains occurred with increases in thickness. Figure 3 shows the weight changes of specimens in the loop as a function of time and temperature, and Fig. 4 shows the overall picture of the mass transfer in the system.

3.2 Specimen Analysis

Figure 5 shows optical micrographs of all the corrosion specimens and some of the loop tubing. Note the attacked areas on the pieces exposed at the higher temperatures and the deposits on the cold leg specimens and the bottom specimen of the hot leg, which also gained weight. It is interesting to note that the weight changes correlate well with the observed microstructural changes. Figure 6 shows micrographs of specimens in the hottest and coldest positions of the loop after 11,900 hr exposure and at the end of the test (19,300 hr). The attacked area is a little more defined after the longer exposure times, and perhaps a few more deposits can be seen.

The two Hastelloy N specimens exposed to the hottest and coldest conditions (Figs. 6*c* and 6*d*) were analyzed by scanning electron microscopy (SEM) and x-ray fluorescence (x-ray fluorescence was induced

14. The repair was successful and the loop was filled with another charge of salt. This "revised" loop was designated NCL-20A and was operated over 2000 hr before termination. However, this report will deal specifically with the results from loop NCL-20.

Table 4. Corrosion specimen data after 19,300 hr exposure

Specimen number[a]	Position[b]	Temperature (°C)	Weight change (mg/cm^2)	Original thickness[c] (mils)	Final thickness[d] (mils)	Observed depth of attack or deposit (mils)
H-01	Hot leg surge tank, vapor BF_3-He	687	−0.3	30.2	30[e]	0
H-02	Hot leg surge tank	687	−5.6	29.3	28	0.5
H-03	Hot leg	687	−14.4	29.4	28[e]	1.0
HM-03[f]	Hot leg	687	−15.5	28.7	26[e]	1.0
H-04	Hot leg	655	−8.9	30.2	29.5	0.5
H-05	Hot leg	620	−2.7	30.9	30.5	0.5
H-06	Hot leg	582	0	30.1	30[e]	0
H-07	Hot leg	555	+2.3	30.3	30.5	0.4
C-01	Cold leg surge tank, vapor BF_3-He	587	−0.4	30.4	30	0
C-02	Cold leg surge tank	587	+0.3	30.0	30	0
C-03	Cold leg	587	+2.8	30.5	30.5	0.5
C-04	Cold leg	544	+4.0	30.9	31.5	0.5
C-05	Cold leg	504	+3.4	30.5	30.5	0.5
C-06	Cold leg	482	+2.7	31.0	31.5	0.5
CM-07[f]	Cold leg	460	+2.0	29.2	29	0.5
C-07	Cold leg	460	+2.8	30.6	31.5	0.5

[a]Specimens H-02 and C-02 in nonflowing salt.
[b]All specimens exposed to molten salt unless noted otherwise.
[c]Measured with a micrometer.
[d]Specimen thickness measured with an optical microscope after specimen mounted for microstructural examination.
[e]Uneven surface.
[f]Modified Hastelloy N.

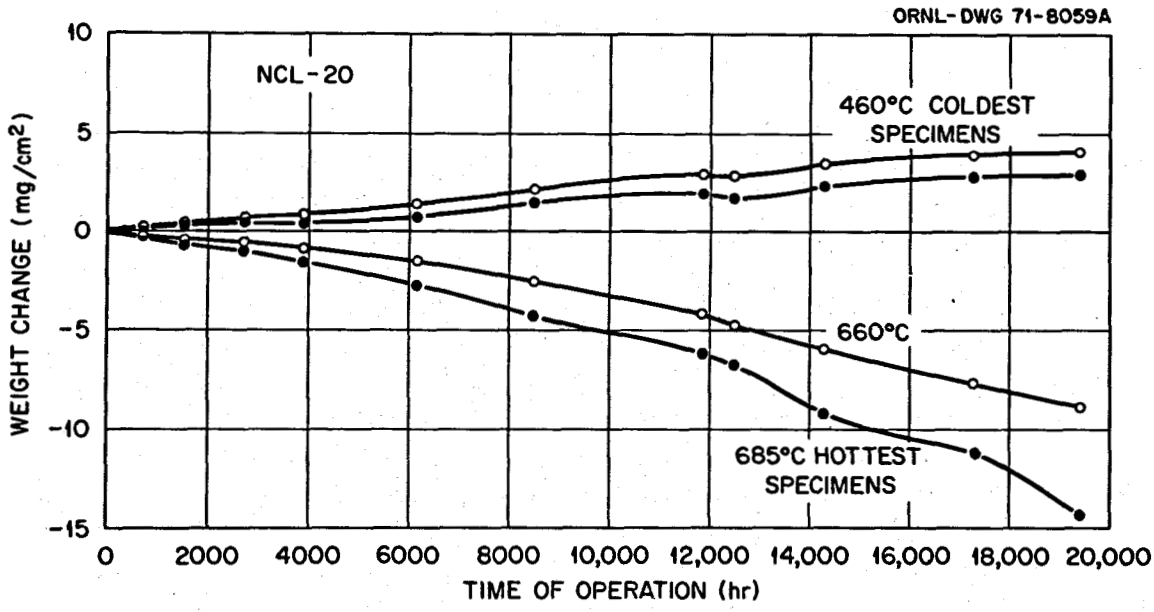

Fig. 3. Weight changes of Hastelloy N specimens from NCL-20 exposed to $NaBF_4$–NaF (92-8 mole %) as a function of time and temperature.

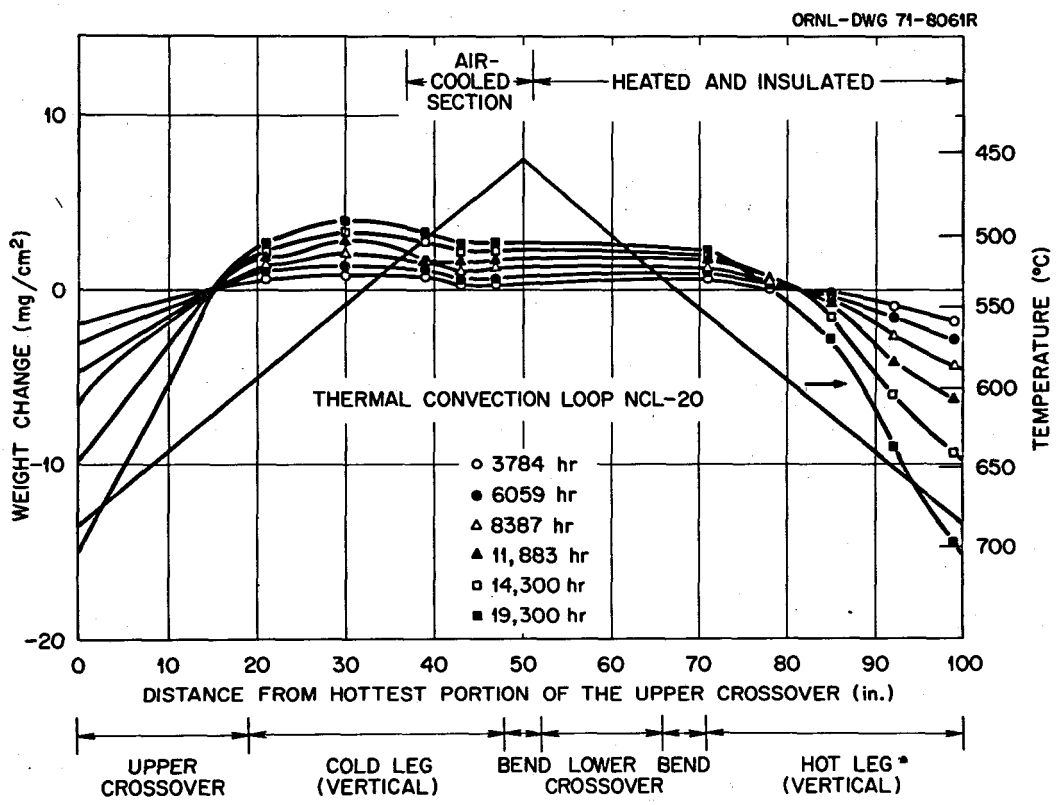

Fig. 4. Weight changes from Hastelloy N specimens in NCL-20 exposed to $NaBF_4$–NaF (92-8 mole %) as a function of position and time.

by bombardment by the electron beam of the SEM).[15] A view of the hot leg specimen at three different magnifications is shown in Fig. 7. The surface has a semipolished appearance. There are many areas which have been undermined with labyrinths of holes and channels. The stereo pairs (Fig. 8) provide a three-dimensional view of the holes and grooves. All areas of Figs. 7 and 8 were composed primarily of nickel and molybdenum. The concentrations of iron and chromium were extremely low. The semiquantitative estimates of concentrations are 71% Ni, 29% Mo, 0.3% Fe, and <0.1% Cr. There were a few areas such as those in Fig. 9 that contained large amounts of debris. The debris is mostly iron, presumably an oxide. Microprobe analysis[16] of specimens after 11,900 hr exposure showed no detectable concentration gradients.

Selected views of the cold leg specimen are shown in Fig. 10. The photos suggest that there has been both dissolution and deposition on this surface. The photos were taken in the area of a plateau on the surface. The grains in this plateau have a flat truncated appearance on top, which suggests that this plateau is part of the original specimen surface that has been only lightly etched. The stereo pairs in Fig. 11 show that the rest of the specimen surface is lower than this plateau. Thus it appears that there has been considerable dissolution of the surface. The concentrations of elements on this surface were 65% Ni, 25% Fe, 0.2% Cr, and 9% Mo. Microprobe analysis of the specimen after 11,900 hr exposure showed that the deposit on the surface was rich in Fe (>25 wt %) and Ni (>64 wt %), but contained very little Cr or Mo.

15. Analysis performed by L. D. Hulett of the Analytical Chemistry Division. Quantitative analysis numbers are subject to errors as high as 20%.

16. Performed by H. Mateer, T. J. Henson, and R. S. Crouse of the Metals and Ceramics Division.

There is also evidence of deposition on the cold leg specimen surface. Figure 12 was taken from an area remote from the plateau. Many of the grains appear to have cubic symmetry. Figures 12*a* and 12*b* show possible growth steps and grains with cubic symmetry. One would not expect the grains of the original alloy substrate to have this much cubic symmetry. The concentrations of elements from the area of Fig. 12 are 65% Ni, 23% Fe, 0.5% Cr, and 11% Mo.

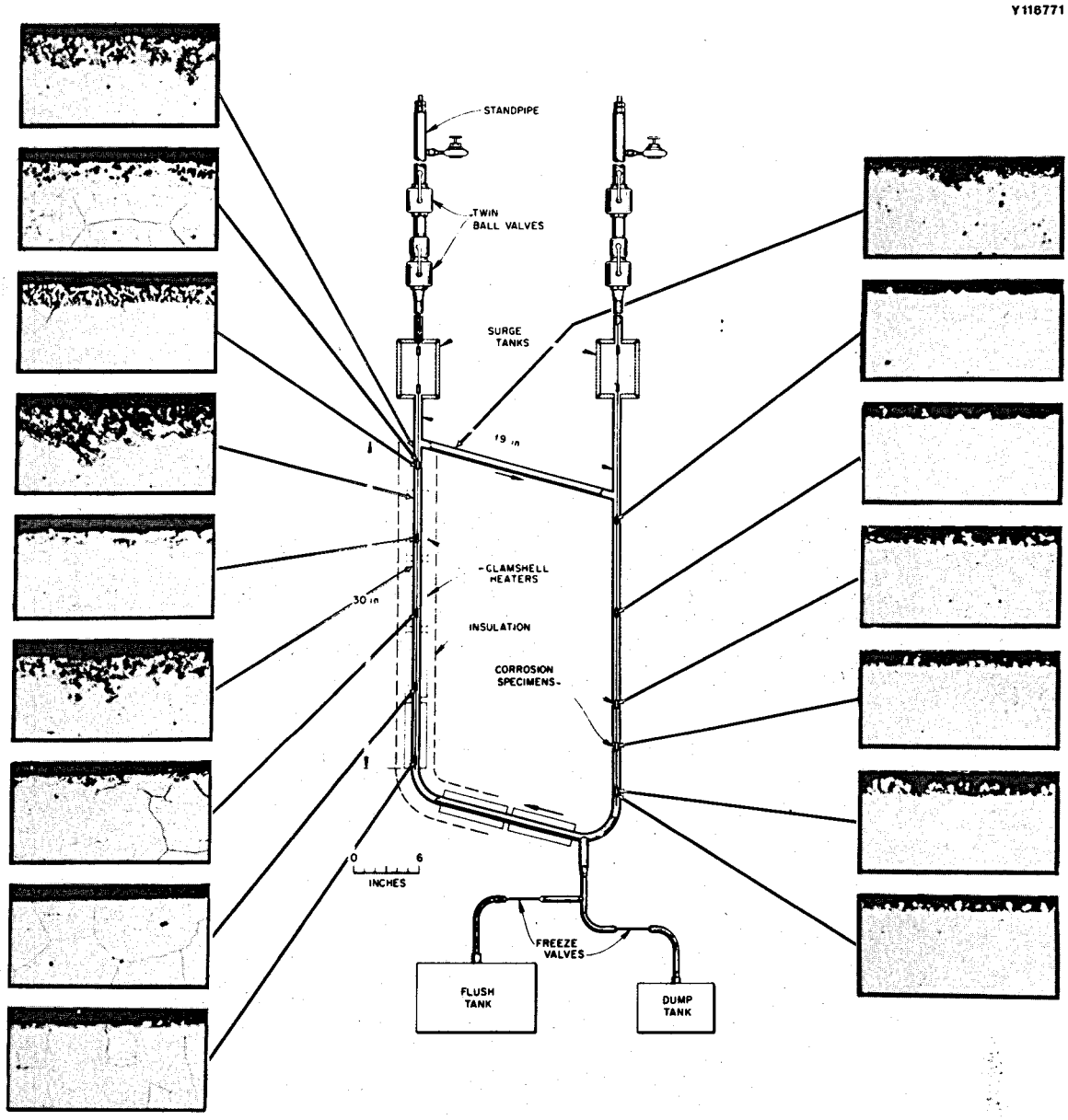

Fig. 5. MSRP natural circulation loop and salt sampler.

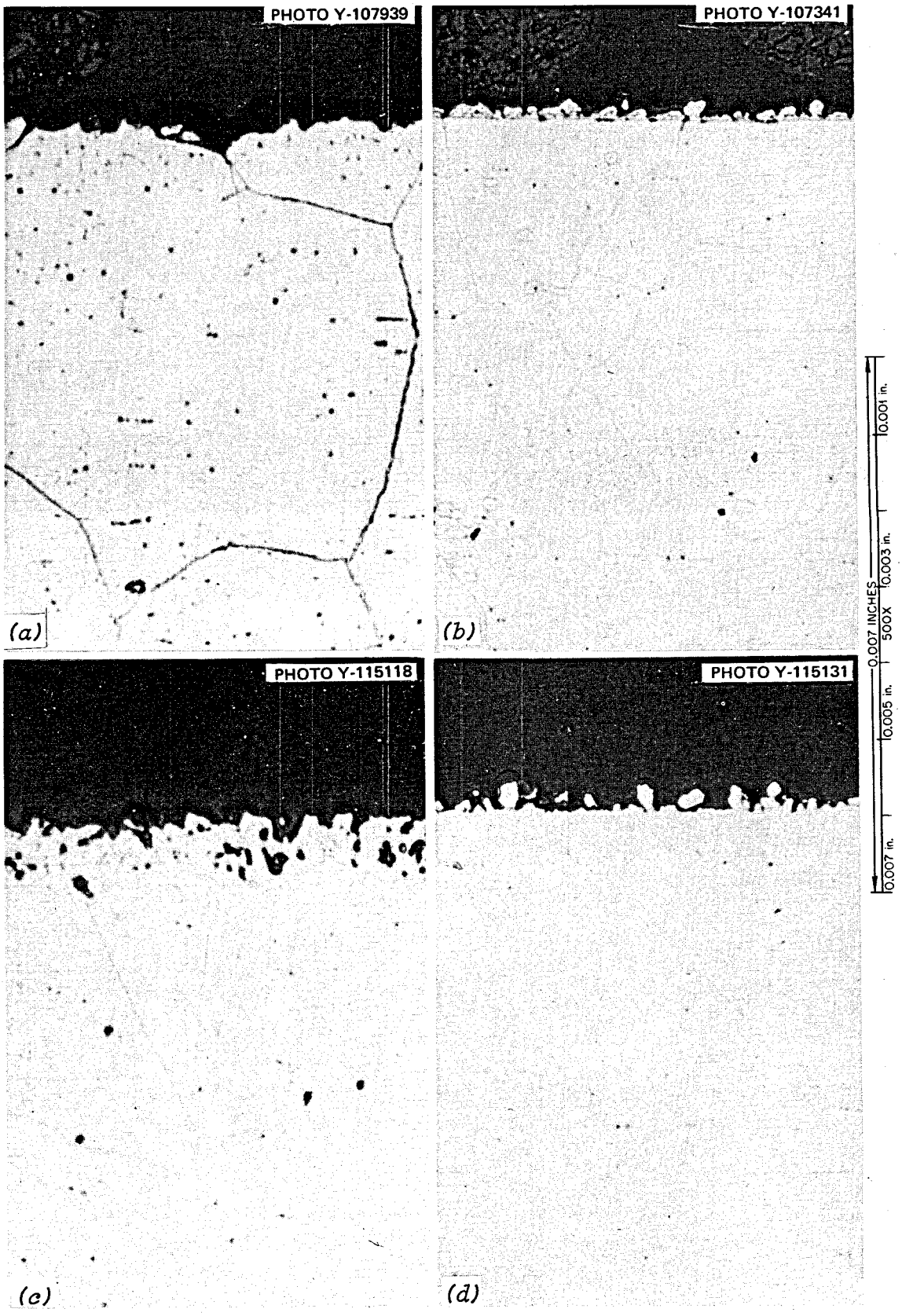

Fig. 6. Optical micrographs of Hastelloy N specimens from NCL-20 exposed to $NaBF_4$–NaF (92–8 mole %). (*a*) 11,900 hr, 685°C, weight loss 6.2 mg/cm^2, etched with glyceria regia; (*b*) 11,900 hr, 460°C, weight gain 2.8 mg/cm^2, as polished; (*c*) 19,300 hr, 685°C, weight loss 14.4 mg/cm^2, etched with glyceria regia; (*d*), 19,300 hr, 460°C, weight gain 4.0 mg/cm^2, as polished.

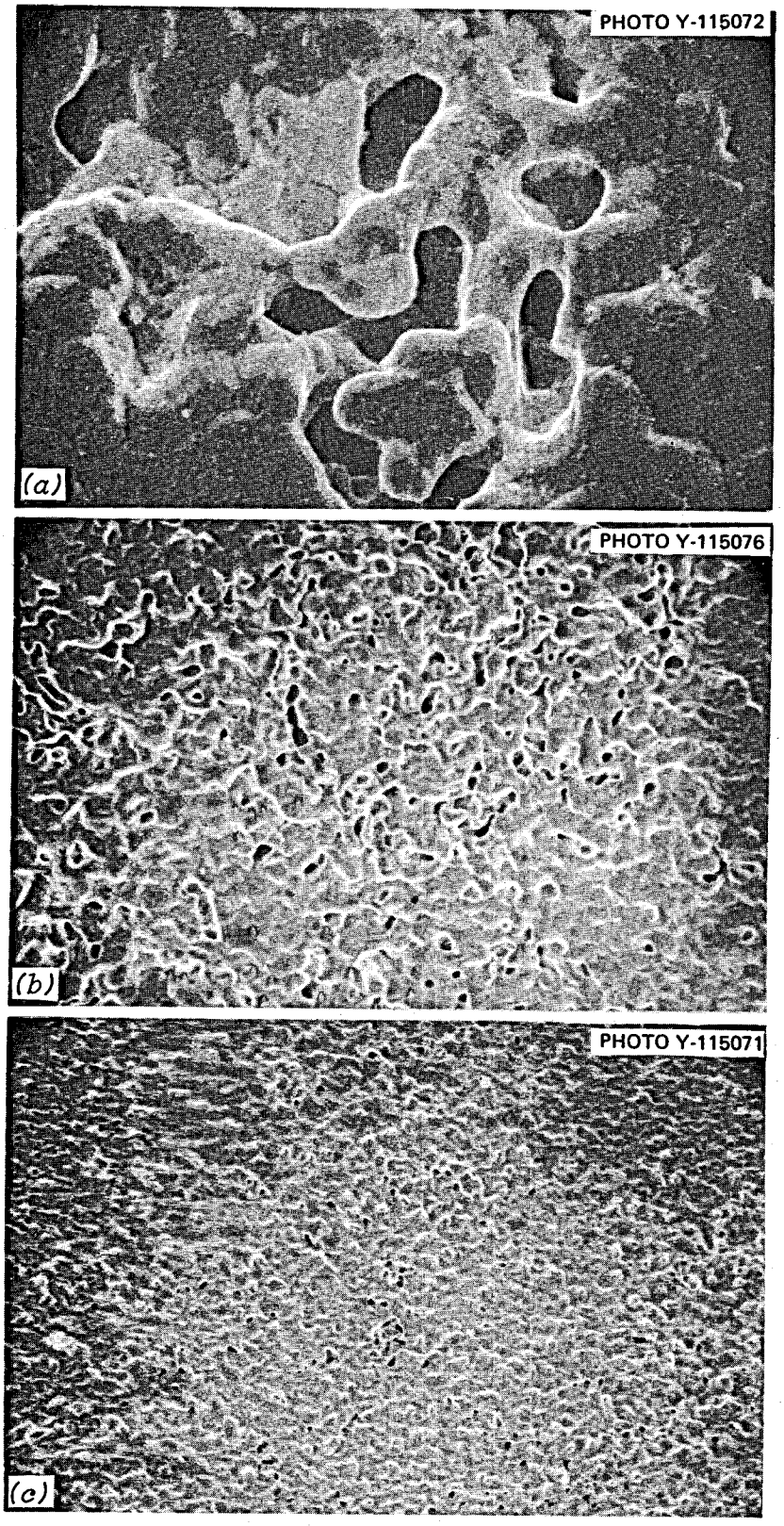

Fig. 7. Scanning electron micrographs of hot leg specimen from NCL-20. (*a*) 5000×; (*b*) 1000×; (*c*) 500×.

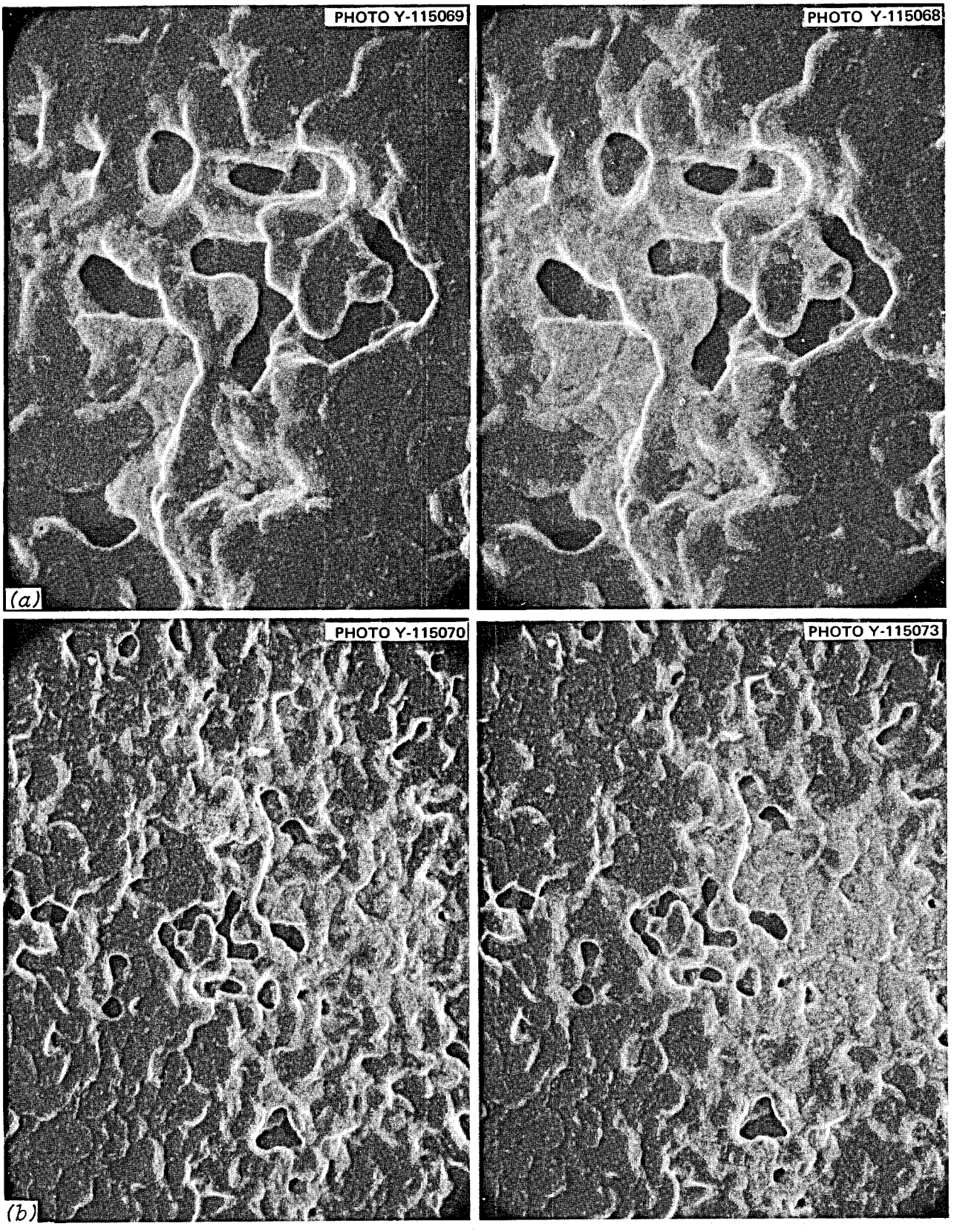

Fig. 8. Scanning electron micrograph stereo pairs of hot leg specimen from NCL-20. (*a*) 5000×; (*b*) 2000×.

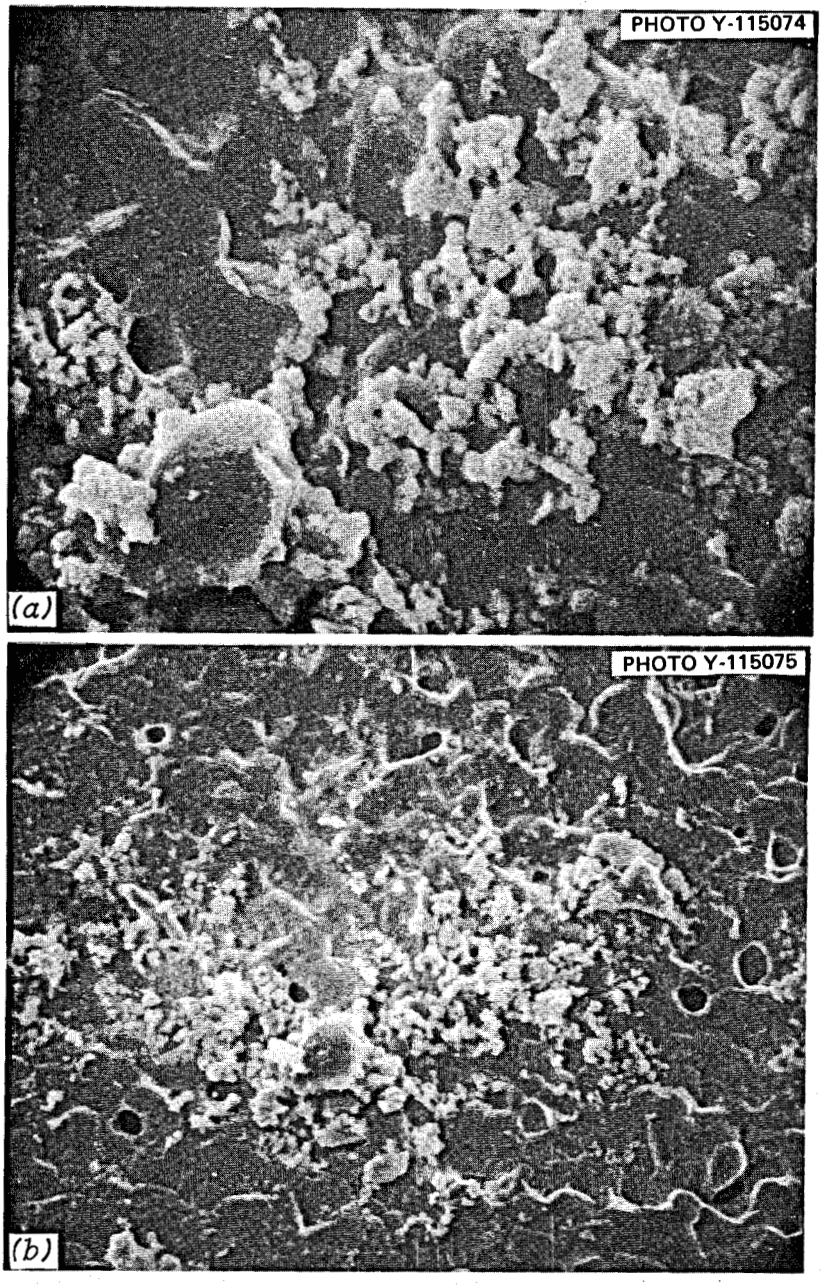

Fig. 9. Scanning electron micrographs of hot leg specimens from NCl-20. (*a*) 5000×; (*b*) 2000×.

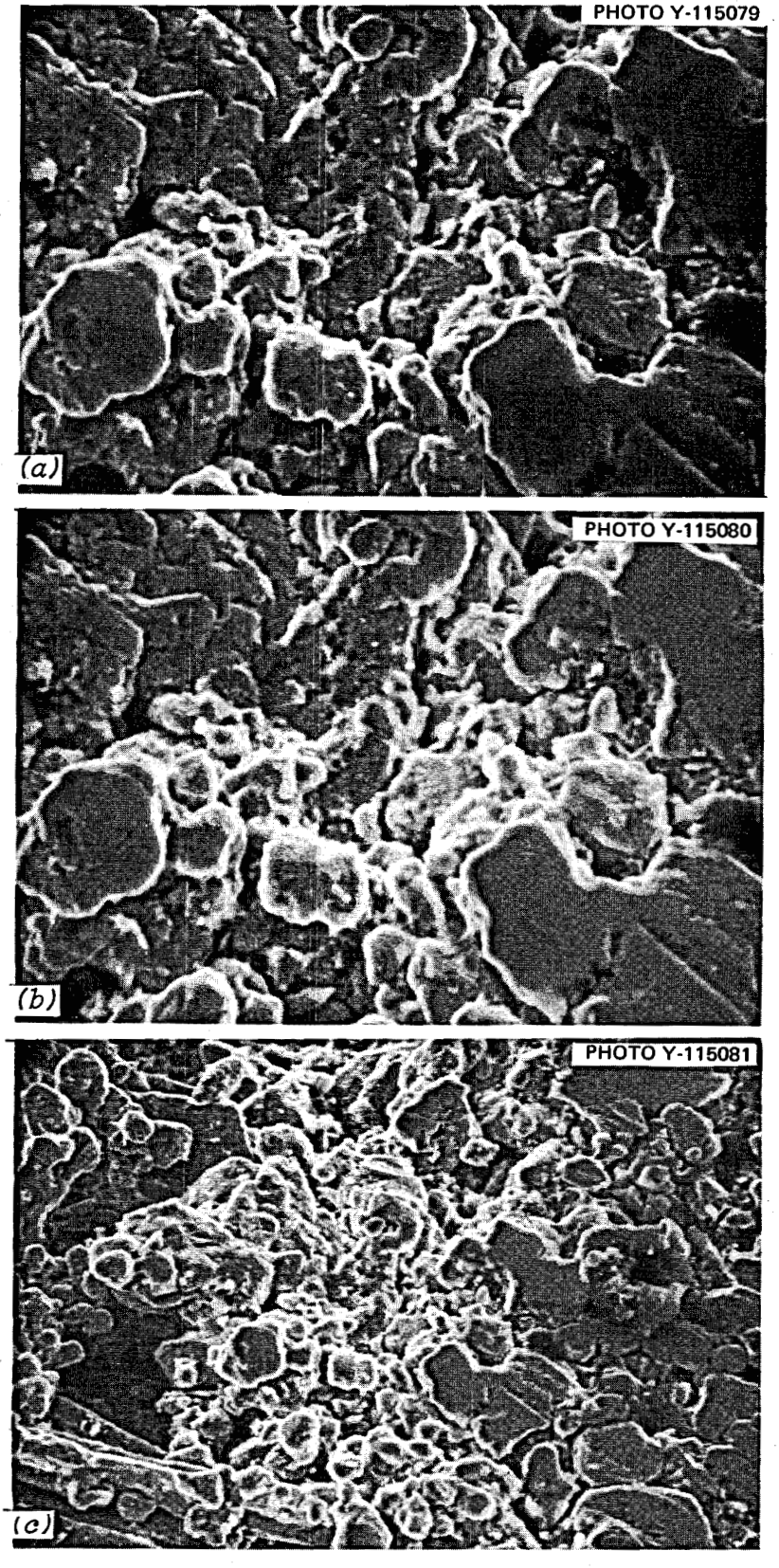

Fig. 10. Scanning electron micrographs of cold leg specimens from NCL-20. (*a*) 10,000×; (*b*) 5000×; (*c*) 2000×.

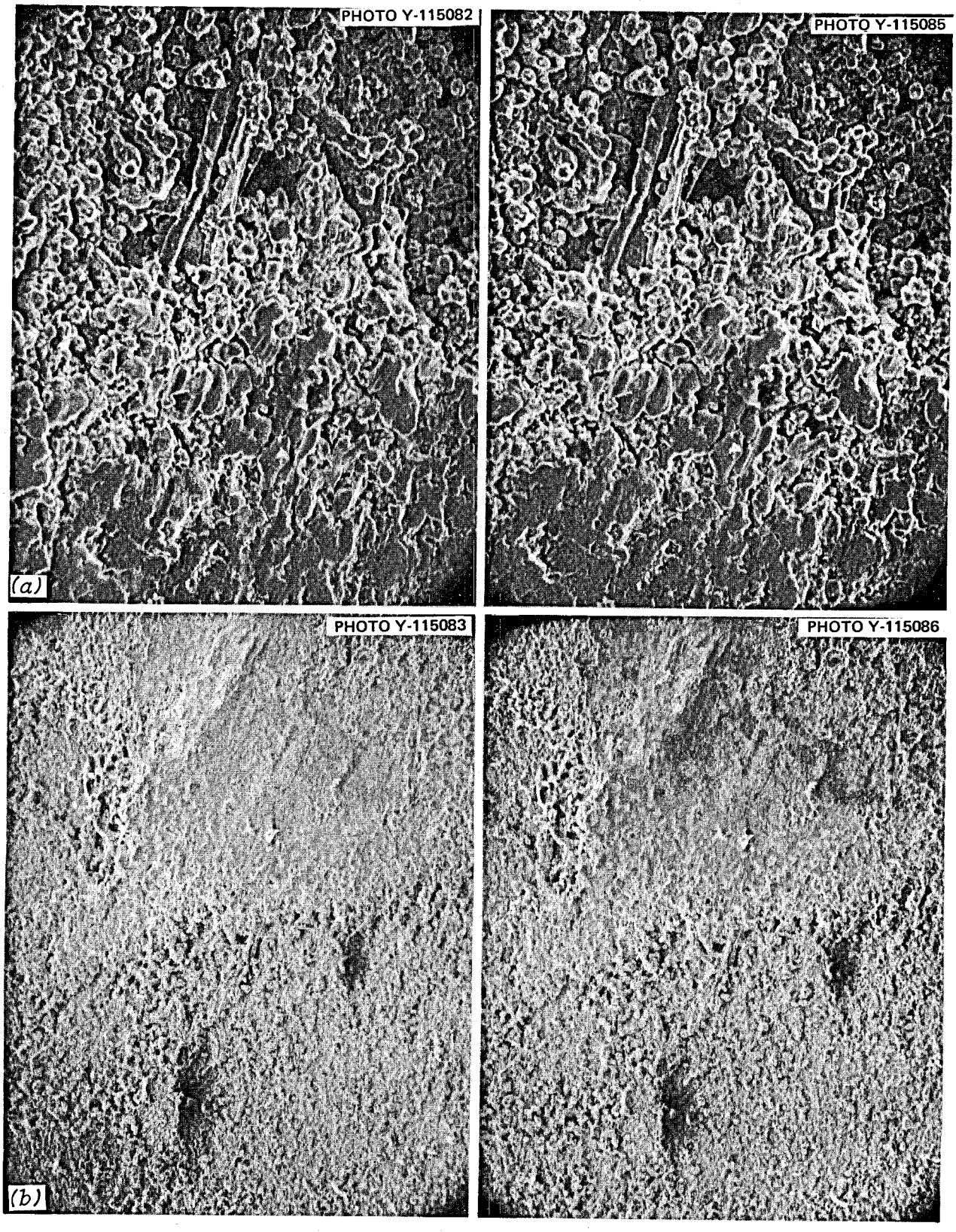

Fig. 11. Scanning electron micrograph stereo pairs of cold leg specimen from NCL-20. (*a*) 1000X; (*b*) 2000X.

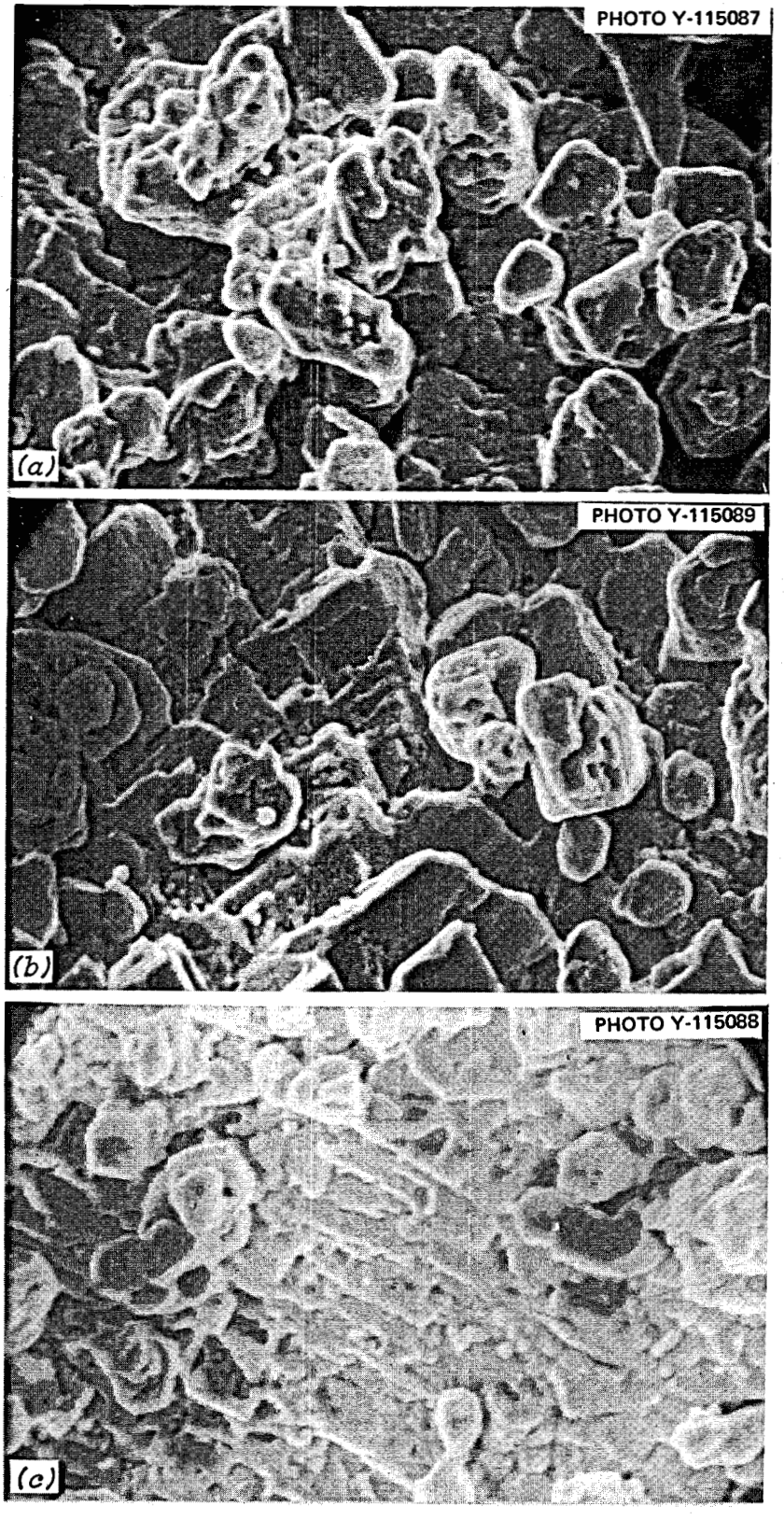

Fig. 12. Scanning electron micrographs of cold leg specimen from NCL-20. (*a*) 5000×; (*b*) 5000×; (*c*) 5000×.

4. DISCUSSION

Temperature-gradient mass transfer, schematically presented in Fig. 13, was seen in this test. As noted in Fig. 4 and the various micrographs, we detected material loss in the hot portions of the loop, material deposition in the cold portion, and a point of little change (balance point) at about 580 or 590°C. Our microprobe analyses showed that iron and chromium were selectively removed in the hot zone. If iron and chromium had been completely removed, the remaining alloy would have contained 80.5% Ni and 19.5% Mo. Analysis showed 71% Ni and 29% Mo; thus some nickel may also have been removed. In the cold leg, assuming that the molybdenum concentration in the alloy had not changed, it appeared that iron and nickel deposited. We also showed that deposition was not entirely a function of temperature, since the weight gains throughout the cold leg varied only a small amount. Thus our picture of mass transfer in this system is that chromium, iron, and smaller amounts of nickel were removed from the hot leg; iron and nickel deposited in the cold leg, and chromium remained in the salt. The corrosion resistance of metals to fluoride fuels has been found to vary directly with the "nobility" of the metal, that is, inversely with the magnitude of free energy of formation of fluorides involving the metal. Accordingly, corrosion of multicomponent alloys tends to be manifested by the selective oxidation and removal of the least-noble component. In the case of Hastelloy N the least-noble constituent is chromium. Iron is more noble than chromium but less than nickel and molybdenum.

In this work, we removed the least-noble constituents, and under conditions where all constituents were removed (formation of Ni, Mo, Fe, and Cr fluorides), the fluorides formed by the noble elements, such as nickel, were so unstable that they were quickly reduced, resulting in iron and nickel deposition in the cold leg.

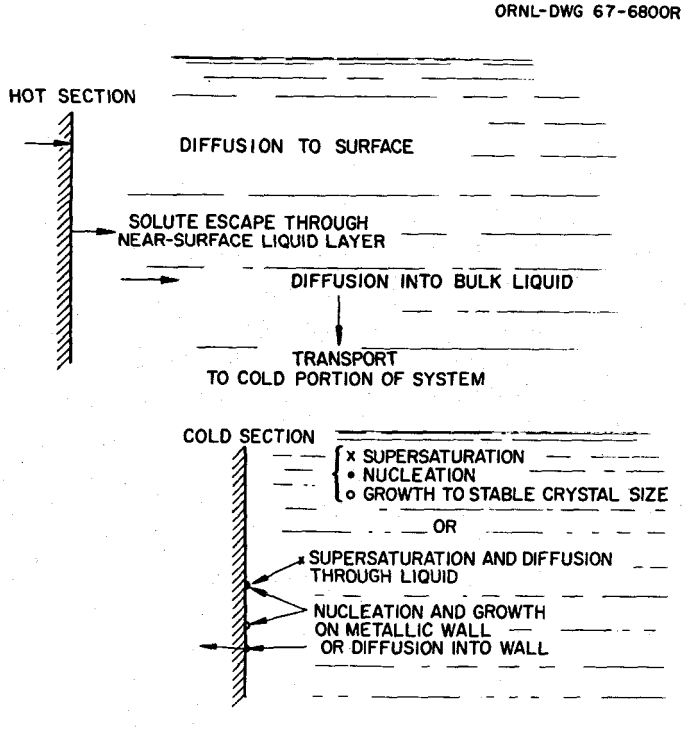

Fig. 13. Temperature-gradient mass transfer.

A large part of the corrosion that occurs in fluoroborate salt is due to impurities, particularly moisture. One of the proposed reactions involves water and fluoroborate as indicated below:

$$H_2O + NaBF_4 \rightleftharpoons NaBF_3OH + HF. \quad (1)$$

The reactions between HF and the metal components of Hastelloy N can be represented by

$$2HF + M \rightleftharpoons MF_2 + H_2, \quad (2)$$

where M = Cr, Fe, Ni, or Mo. In our system the most predominant expression of Eq. (2) is, therefore,

$$6HF + 2Cr + 6NaF \rightleftharpoons 2Na_3CrF_6 + 3H_2, \quad (2a)$$

although nickel and iron also react with HF.

The effect of HF in a salt system can be quite virulent. A previous Hastelloy N loop that circulated equimolar $NaF\text{-}ZrF_4$ salt saturated with HF operated only 200 hr before it became plugged with nickel corrosion product.[17] Attack of the Hastelloy N in this case was uniform throughout the loop.

We noted increased attack when we had impurity inleakages of air and moisture.

It is also thought that the hydroxide compound from Eq. (1) may dissociate in the following manner:

$$NaBF_3OH \rightleftharpoons NaBF_2O + HF. \quad (3)$$

Combining reactions (1), (2*a*), and (3) we get

$$6NaF + 3NaBF_4 + 3H_2O + 2Cr \rightleftharpoons 3NaBF_2O + 2Na_3CrF_6 + 3H_2. \quad (4)$$

Reactions (2a) and (3) can be combined to obtain

$$6NaF + 6NaBF_3OH + 2Cr \rightleftharpoons 6NaBF_2O + 2Na_3CrF_6 + 3H_2. \quad (5)$$

Removal of hydrogen from the system by diffusion would drive reactions (4) and (5) to the right.

In fluoride salt systems, the temperature-gradient mass transfer process begins with material removal at all temperatures, and later, as the corrosion product concentration increases, deposition begins in the colder sections. We assume that the mass transfer in our system occurred in the same manner as described above, with primarily chromium removal with some iron dissolution also. Thus we can explain that the dissolution and deposition that occurred in the cold leg (as seen in the SEM) stemmed from material removal all over the loop before equilibrium was attained at the lowest temperature point. After equilibrium, the chromium then was returned to the walls in the cold part of the system.

Since the weight losses of the hottest specimen are functions of time, they can be fitted to an equation of the type

$$W = at^b,$$

17. *MSR Program Semiannu. Progr. Rep. Feb. 28, 1962,* ORNL-3282, p. 72.

where

W = weight loss in milligrams per square centimeter of surface area,

a = a constant,

t = time in hours, and

b = a kinetic time constant.

For a solid-state diffusion-controlled process, $b = \frac{1}{2}$, and for a dissolution-controlled process $b = 1$ (ref. 18). Calculations showed that for the first 11,900 hr $a = 2 \times 10^{-4}$ and $b = 1.1$. The almost straight-line dependence of weight loss with time ($b = 1.1$) also points to a fairly general type of attack, as opposed to selective removal of only one element. The salt analysis showed evidence of reaction (1) in that an ionic species of iron was removed from the salt while the concentration of chromium ions increased. Thus in keeping with our other findings it would appear that more iron deposited than was removed.

Subsurface voids are often formed in alloys exposed to molten salts, and we see them in some of our hot leg specimens. The formation of these voids is generally initiated by the selective oxidation of an alloy constituent (usually chromium) along exposed surfaces through oxidation-reduction reactions with impurities or constituents of the molten fluoride mixture. As the surface is depleted in chromium (or the least-noble constituent), chromium from the interior diffuses down the concentration gradient to the surface. Since diffusion occurs by a vacancy process and in this particular situation is essentially unidirectional, it is possible to build up an excess number of vacancies in the metal. These precipitate in areas of disregistry, and voids tend to agglomerate and grow in size with increasing time and/or temperature. Examinations have demonstrated that the subsurface voids are not interconnected with each other or with the surface. Voids of this same type have also been developed in Inconel by high-temperature oxidation tests and high-temperature vacuum tests in which chromium is selectively removed.[19] Voids similar to these have also been developed in copper-brass diffusion couples and by the dezincification of brass.[20] All of these phenomena arise from the so-called Kirkendall effect; that is, solute atoms of a given type diffuse out at a faster rate than other atoms comprising the crystal lattice can diffuse in to fill vacancies that result from the outward diffusion. In our case the attack was selective toward iron and chromium, and still voids were seen. Thus void formation does not mean that only one element has been removed from the alloy matrix.

5. CONCLUSIONS

1. Temperature-gradient mass transfer of Hastelloy N, exposed to a sodium fluoroborate mixture of $NaBF_4$–8 mole % NaF in a thermal convection loop system that operated at temperatures of 687°C maximum and 438°C minimum for 19,930 hr, does occur. The maximum calculated corrosion rate (based on uniform removal) was 0.29 mil/year.

2. Material removal (chromium and iron) that resulted in voids occurred in the hot leg while iron and nickel deposited in the cold section with chromium ions remaining in the salt.

3. Some of the deposits in the cold leg appeared to have cubic symmetry.

4. Impurities in the loop system (probably stemming from air inleakage) increased the mass transfer rate.

5. Overall, the compatibility in this system was quite good.

---

18. J. W. Koger, *Corrosion and Mass Transfer Characteristics of $NaBF_4$-NaF (92-8 Mole %) in Hastelloy N*, ORNL-TM-3866, October 1972, pp. 66–68.

19. A. DeS. Brasunas, "Sub-Surface Porosity Developed in Sound Metals During High-Temperature Corrosion," *Metals Progr.* 62(6), 88 (1952).

20. R. W. Balluffi and B. H. Alexander, "Development of Porosity by Unequal Diffusion in Substitutional Solutions," SEP-83, Sylvania Electric Products (February 1952).

INTERNAL DISTRIBUTION

(79 copies)

(3) Central Research Library
ORNL – Y-12 Technical Library
Document Reference Section
(10) Laboratory Records Department
Laboratory Records, ORNL RC
ORNL Patent Office
G. M. Adamson, Jr.
C. F. Baes
C. E. Bamberger
S. E. Beall
E. G. Bohlmann
R. B. Briggs
S. Cantor
E. L. Compere
W. H. Cook
F. L. Culler
J. E. Cunningham
J. M. Dale
J. H. DeVan
J. R. DiStefano
J. R. Engel
D. E. Ferguson
J. H. Frye, Jr.
L. O. Gilpatrick
W. R. Grimes
A. G. Grindell
W. O. Harms
P. N. Haubenreich
(3) M. R. Hill
W. R. Huntley
H. Inouye
P. R. Kasten
(5) J. W. Koger
E. J. Lawrence
A. L. Lotts
T. S. Lundy
R. N. Lyon
H. G. MacPherson
R. E. MacPherson
W. R. Martin
R. W. McClung
H. E. McCoy
C. J. McHargue
H. A. McLain
B. McNabb
L. E. McNeese
A. S. Meyer
R. B. Parker
P. Patriarca
A. M. Perry
M. W. Rosenthal
H. C. Savage
J. L. Scott
J. H. Shaffer
G. M. Slaughter
G. P. Smith
R. A. Strehlow
R. E. Thoma
D. B. Trauger
A. M. Weinberg
J. R. Weir
J. C. White
L. V. Wilson

EXTERNAL DISTRIBUTION

(24 copies)

BABCOCK & WILCOX COMPANY, P. O. Box 1260, Lynchburg, VA 24505
B. Mong

BLACK AND VEATCH, P. O. Box 8405, Kansas City, MO 64114
C. B. Deering

BRYON JACKSON PUMP, P. O. Box 2017, Los Angeles, CA 90054
G. C. Clasby

CABOT CORPORATION, STELLITE DIVISION, 1020 Park Ave., Kokomo, IN 46901
T. K. Roche

CONTINENTAL OIL COMPANY, Ponca City, OK 74601
J. A. Acciarri

EBASCO SERVICES, INC., 2 Rector Street, New York, NY 10006
D. R. deBoisblanc
T. A. Flynn

THE INTERNATIONAL NICKEL COMPANY, Huntington, WV 25720
J. M. Martin

UNION CARBIDE CORPORATION, CARBON PRODUCTS DIVISION, 12900 Snow Road, Parma, OH 44130
R. M. Bushong

USAEC, DIVISION OF REACTOR DEVELOPMENT AND TECHNOLOGY, Washington, DC 20545
David Elias
J. E. Fox
Norton Haberman
C. E. Johnson
T. C. Reuther
S. Rosen
Milton Shaw
J. M. Simmons

USAEC, DIVISION OF REGULATIONS, Washington, DC 20545
A. Giambusso

USAEC, RDT SITE REPRESENTATIVES, Oak Ridge National Laboratory, P. O. Box X, Oak Ridge, TN 37830
D. F. Cope
Kermit Laughon
C. L. Matthews

USAEC, OAK RIDGE OPERATIONS, P. O. Box E, Oak Ridge, TN 37830
Research and Technical Support Division

USAEC, TECHNICAL INFORMATION CENTER, P. O. Box 62, Oak Ridge, TN 37830
(2)